

Basic Investigations

Study on the Protective Effect of Shengmai San (生脉散) on the Myocardium in the Type 2 Diabetic Cardiomyopathy Model Rat

NI Qing 倪青¹, WANG Jie 王阶¹, LI En-qing 李恩庆², ZHAO An-bin 赵安斌², YU Bin 于斌²,
WANG Min 王敏², and HUANG Chun-rong 黄春荣²

Objective: To study the effect of Shengmai San (生脉散 Pulse-activating Powder) in protecting myocardium in the rat of the type 2 diabetic cardiomyopathy (DCM) model.

Methods: The DCM rat model was established by combination of insulin resistance induced by a high-fat diet with intraperitoneal injection of high dose streptozotocin (50 mg/kg). And these rat models were randomly divided into three groups: a normal group ($n=12$, one of them died), a model group ($n=15$) and a Shengmai San group (treatment group, $n=15$). The damage of the myocardium was assessed by electrocardiogram at the twelfth week after modeling, and the blood glucose, cholesterol and triglyceride levels were determined; the content of the left cardiac ventricle myocardial collagen was quantified by Masson staining test; the level of myocardial cell apoptosis was detected with TUNEL apoptosis detection kit; the damage extent of the myocardial sub-cellular structures was observed by electron microscopy; the expression levels of cardiac TSP-1 (Thrombospondin-1), TGF- β 1 (Transforming Growth Factor- β) and TRB-3 (Tribbles homolog 3) proteins were detected by immunohistochemical method; the expression levels of cardiac TSP-1, A-TGF- β 1 and L-TGF- β 1 proteins were detected by Western blotting; and the expression levels of TSP-1 and TRB-3 mRNAs were detected by real-time quantitative PCR.

Results: Compared with the control group, the blood glucose, cholesterol, triglycerides levels in both the model groups and the Shengmai San group were significantly decreased; the myocardial tissue was less damaged and the collagen content was reduced in the Shengmai San group; the myocardial sub-cellular structure was injured to a lesser extent; the expression levels of myocardial TSP-1, TGF- β 1, TRB-3, and TSP-1, A-TGF- β 1, L-TGF- β 1 and chymase were decreased, and the expression levels of TSP-1 mRNA and TRB-3 mRNA were decreased in both the model groups and the Shengmai San group (the latter was better).

Conclusion: Shengmai San can inhibit myocardial fibrosis in the rat of diabetic cardiomyopathy, and significantly delay the formation of diabetic cardiomyopathy in hyperglycemia rats through multiple pathways.

Keywords: Shengmai San; diabetic cardiomyopathy; collagen fiber; apoptosis; TSP-1; TGF- β 1; TRB-3; Chymase

Diabetic cardiomyopathy (DCM) is a special myocardial disease caused by diabetes and occurs alone or is accompanied with vascular diseases, which is referred to a primary myocardial cell injury with extensive structural abnormalities in diabetics and ultimately leads to left ventricular hypertrophy, diastolic and/or systolic dysfunction, and it has chronic pathological changes due to acute responses of myocardium to diabetes.^{1,2} In clinic, its early manifestation may be diastolic heart failure,^{3,4} i.e., myocardial relaxation reduction and stiffness increase, and interstitial fibrosis of myocardium may play an important pathogenic role in diastolic heart failure.^{5,6} In histomorphology, it manifests mainly as focal myocardial hypertrophy, necrosis, extracellular matrix (ECM) deposition and myocardial fibrosis.^{7,8} Seventy percent of diabetics die of cardiovascular diseases, the mortality being 2-3 times of that in the people without diabetes.⁹ Since Shengmai San (生脉散 Pulse-activating Powder) is found to be of the higher frequency of use by data-mining in 1278 cases of multi-center diabetic in-patients with coronary heart disease, therefore, study on the therapeutic effects of Shengmai San on diabetic myocardial fibrosis may provide instruction for its clinical use.

MATERIALS AND METHODS

Main Reagents and Instruments

Trizol was purchased from Invitrogen Biotechnology Company; RNA reverse transcription kit from Shanghai Beibo Biotechnology Company; real-time quantitative PCR kit from Genecopoeia Biotechnology Company; TSP-1 (Thrombospondin-1), TGF- β 1 (Transforming Growth Factor- β), TRB-3 (Tribbles homolog 3) and Chymase monoclonal antibody from Santa Cruz Biotechnology Company, USA; A-TGF- β 1 and L-TGF- β 1 polyclonal antibody from Wuhan Boster Biological Technology Company; ABC detection kit from Vectro Biotechnology Company, USA; BCA

1. The Endocrinology department of Guang'anmen Hospital of China Academy of Chinese Medical Sciences, Beijing 100053, China; 2. School of Medicine, Jinan University, Guangzhou 510632, China

Correspondence to: Prof. WANG jie, Email: wangjie@163.com

This study was financially supported by the first grade grant (No. 200070410129) and the first batch special grant (No. 200801166) from China Postdoctoral Science Foundation, and the major project (No. H020920010330), and the subject of Science and Technology Plan of Beijing Science and Technology Commission (No. D08050703020802).

protein kit from Shanghai Beibo Biological Reagent Company; and Streptozotocin (STZ) from Sigma Biotechnology Company; Shengmai San was purchased from the Traditional Chinese Medicine Department of the First Affiliated Hospital of Jinan University, which consists of Ren Shen (Radix Ginseng) 9 g, Mai Dong (Radix Ophiopogonis) 9 g, and Wu Wei Zi (Fructus Schisandrae) 6 g. After Mai Dong and Wu Wei Zi were decocted with 10 times of water for 1.5 h, and Ren Shen was elsewhere decocted with 10 times of water for 1.5 h, the two decoctions were filtered and mingled together, and after another filtration, the solution was concentrated as 0.32 g/mL.

Experimental Animals and Grouping

Forty-two male SD rats (of the second grade, i.e. Clean animals), with body weight of (200 ± 20) g, purchased from Beijing Vital River Laboratory Animal Technology Co., Ltd., were randomly divided into 3 groups with random number chart: a normal group ($n=12$), a model group ($n=15$) and a Shengmai San group (treatment group, $n=15$). The rats in the normal group were fed with a standard diet, and those in the model group and the Shengmai San group were fed with high fat and high calorie diet. After 4 weeks, an intraperitoneal injection of STZ (50 mg/kg) was given to every rat of the model group and the Shengmai San group, while the rats of the normal group received intraperitoneal injection of the same dose of sodium citrate buffer; and then the rats in each group were fed with the original feed. One week later, blood glucose is checked, and those with two consecutive blood glucose ≥ 16.7 mmol/L and polydipsia, polyphagia and polyuria in the model group and in the Shengmai San group were included in the experiment, 13 rats in the model and 13 rats in the Shengmai San group. The rats were fed with the original feed for 9 weeks, and Shengmai San 7.5 mL/kg was intragastrically administrated for the Shengmai San group and the equivalent distilled water for the model group each day. After 12-h fasting, 4 rats of each group were killed by Decapitated method at the 8th week, 11th week, and 14th week of the experiment respectively to take blood from their atriums, which was then centrifugated and the serum was stored in -20°C for further tests of blood lipids and blood glucose, and the hearts were rapidly taken and then rinsed with ice salt water, the capsule and the blood vessels were cut off, and the hearts were weighed for calculating the heart weight index; and the myocardium in the upper and lower parts of the symmetrical mid-point along the perpendicular line of the long axis in the left ventricle were taken and placed respectively in the 10% neutral formaldehyde and 2.5% glutaraldehyde, and the residual part of myocardium was placed in a refrigerator at -80°C . Thirty-five rats had completed the study (One rat in the model group died of possible complications of diabetes or infection).

Electrocardiogram Observation for Myocardial Damage

Electrocardiogram was taken for each rat after an intraperitoneal injection of 1% sodium pentobarbital (2 mL/kg).

Detection of Total Cholesterol, Triglyceride and Blood Sugar

Atrium blood 5 mL was centrifugated at 2500 r/min, 4°C and the serum was stored at -20°C for tests of serum blood lipids and blood glucose.

HE Staining

Myocardial tissue samples fixed in 10% neutral formalin were made paraffin sections and routine HE staining was carried out. The myocardial injuries were observed and photographed, and then in combination with the ultrastructural changes, the myocardial lesions were evaluated.

Transmission Electron Microscope (TEM)

After fixed in 2.5% glutaraldehyde for 10 min, the small pieces of tissue from the middle of the left ventricle were finely cut ($1.0\text{ mm} \times 1.0\text{ mm}$) and fixed for another 12 h, then fixed with 1% osmic acid for 1 h, followed by gradient dehydration with ethanol and acetone, epoxy resin embedding, the preparation of thin sections with ultramicrotome, electron staining, and observation for myocardial ultrastructures and photography with the Germany PHILIPSTECNAI-10 type transmission electron microscopy.

Masson Staining

After conventional deparaffin of the paraffin sections, Masson staining was made. The myocardial cells were red or yellow and the collagen fibers were blue and green under light microscopy; the CVF in each view of the slices was quantitatively analyzed with HMIAS color medical analysis system ($\text{CVF} = \frac{\text{the collagen area in the same image}}{\text{measured vision area}}$) and the area of blood vessels rich in collagen and scar were excluded. For each slice, five views were selected and finally the mean was calculated.

Cell Apoptosis Detection with TUNEL Apoptosis Detection Kit

After deparaffin of the conventional paraffin sections and the reagents were dropped in order following the kit instructions, and they were observed under fluorescence microscope with excitation wavelength of 450-500 nm and emission wavelength of 515-565 nm. Three to five fields of view with the strongest fluorescence expressions in each slice were selected and observed by the scanning and analysis software in the computer to check the fluorescence intensity and the area. The fluorescence value of index = mean fluorescence intensity \times mean fluorescence area.

Real-time Quantitative PCR

RNA extraction and cDNA synthesis were made according to the kit instructions. The RNA was extracted with Trizol, and the purity and the concentration of RNA were detected by UV spectrophotometer and the integrity was checked by electrophoresis. The reverse transcription was done according to the kit instructions. Two μL reverse transcription products were taken for Real-time PCR detection.

Primer sequence: primer was synthesized and provided

by the Shanghai Biological Engineering Technology Services Co. Ltd.

Table1. List of the genes and the primers involved in this study

Target gene	Primer sequence (5'-3')	Product length (bp)
TRB-3	F: TGTCTTCAGCAACTGTGAGAGGACGAAG R: GTAGGATGGCCGGGAGCTGAGTATC	147
Tsp-1	F: GGAAGAGC ATCACGCTGTTTG R: GCGCTCTCCATCTTGTCACA	73
β-actin	F: GACATCCGTAAAGACCTCTATGCC R: ATAG AGCCACCAATCCACACAGAG	173

Reaction system: 2 × Allinone™ Q-PCR MIX 10 μL, ddH₂O 1 μL, Forward Primer (4 μmol/L) 2 μL, Reverse primer (4 μmol/L) 2 μL, Template cDNA 5 μL. Total: 20 μL.

Reaction conditions: denaturation: 95 °C, 1 min; denaturation: 95 °C, 15 second; annealing: 60 °C, 30 second; extension: 72 °C, 30 second. A total of 40 cycles.

Immunohistochemical Staining

The slides were carried out for anti-shedding treatment by Polylysine, followed by routine deparaffin, and blockade by 0.3% H₂O₂ and then were put into 0.01 mol/L pH 6.0 citrate buffer to repair antigen in microwave (mid-range fire, 8-10 min, then cooling to room temperature, repeated 3 times). After sealed by the goat serum, antibody-I, biotin-labeled goat-anti-mouse IgG and horseradish-peroxidase-labeled egg protein-biotin were added successively and incubated at 37 °C for 30 min, coloration with DAB (3,3'-diaminobenzidine), dehydration, transparency and enclosure of the slice. For the negative control, PBS replaced the antidody-I. With the Leica Qwin Plus Analysis system, the stained pictures were analyzed, and five unrepeatable positive reaction views were randomly selected in each slice and taken pictures, and their average gray value was calculated.

Protein Expression Detection by Western Blotting

On the ultra-clean table, 100 mg tissue was clipped and ground on ice after 400 μL cell lysate was added, and then transferred to 1.5 mL Eppendorf tube for lysis on ice for 30 min; after centrifugation at 12 000 r/min and 4 °C for 10 min, the supernatant (the protein sample) was taken and transferred to 1.5 mL centrifuge tubes, and stored in a refrigerator at -80 °C. Forty μL such protein samples were taken to quantify the protein with BCA kit and the standard curve was drawn. The protein samples (20 μg), after electrophoresis in 10% polyacrylamide gel, was transferred (wet transfer), with constant current (GAPDH: 240 MA, 50 min; tsp-1: 240 MA, 140 min), onto the PVDF membrane (pore size 0.45 μm), and after closed with buffer (5% skim milk or BSA) for 1 h. Then the membrane was put into the antibody-I diluted with closed buffer (dilution ratio: GAPDH: dilution of 1:100, TSP-1: of 1:200; A- TGF-β1: of 1:100; L-TGF-β1: of 1:100) for the immunological reaction in a

continuous shaking incubation at a room temperature for 2 h, and then settled overnight at 4 °C. After that, the membrane was rinsed by 1 × PBST for four times and 5 min each time, and then incubated with the Horseradish peroxidase (HRP) labeled antibody-II diluted by PBST buffer (dilution of 1:6000) at room temperature for 50 min, and rinsed by 1 × PBST for another four times and 5 min each time. In the dark room, the membrane was added with 0.6 mL freshly prepared ECL chromogenic solution (equal volume mixing of fluid A and fluid B) and incubated for 1 min, and then sealed in a preservative membrane, pressed, and developed to the photosensitive film. Repeated the above steps 3 times independently. With the Bandleader 3.0 software, the bands went through gray scale scanning, and according to the following formula, the relative content of protein samples in these 3 experiments were calculated respectively the relative content of protein (the gray value of the protein bands minus the gray value of the background) / (the gray value of the band of the internal reference minus the gray value of the background), thereby the mean and standard deviation of the ratio can be calculated.

Statistical Analysis

All data were analyzed with SPSS13.0 software. Quantitative data was expressed by means ± standard deviation ($\bar{x} \pm s$). The single factor analysis of variance of completely randomized design was used for the parameter comparison between groups. The level for signification is $P < 0.05$ or < 0.019 .

RESULTS

Changes of the General Living States and Biochemical Indexes of Rats

The diabetic model rat showed polydipsia, polyuria, polyphagia symptoms within one week after STZ injection, and with the disease duration went longer, these symptoms gradually aggravated and more symptoms appeared, including abdominal swelling, severe weight loss, diarrhea, dry hair, dark color, torpid reaction, less activity, and rough respiratory sound in part of the rats. With time prolonged, both the serum triglyceride and the total cholesterol levels in the model group and the Shengmai San group gradually increased with significant differences in different longitudinal time points among these different groups (The F values of triglyceride in the model group and in the Shengmai San

group were respectively 25.429 and 0.825, both $P < 0.05$; and the F values of total cholesterol in the model group and in the Shengmai San group were 9.065 and 0.098, both $P < 0.05$; the blood glucose decreased in both the model group and the Shengmai San group at different time points, with no statistically significant differences (all $P > 0.05$). The comparisons of the serum triglyceride and the serum total cholesterol levels between different time points in the normal group are all of no significant differences (all $P > 0.05$); Compared with the normal group, the serum triglyceride and the serum total cholesterol levels in both the model group and the

Shengmai San group were significantly increased; Compared with the model group in the same time point, the serum triglyceride and the serum total cholesterol levels in the Shengmai San group significantly decreased with significant differences ($P < 0.01$); Compared with the normal group in the same time point, the serum glucose levels in both the model group and the Shengmai San group were significantly increased; And compared with the model group in the same time point, the serum glucose levels in the Shengmai San group were significantly decreased with significant differences ($P < 0.05$, Figure 1).

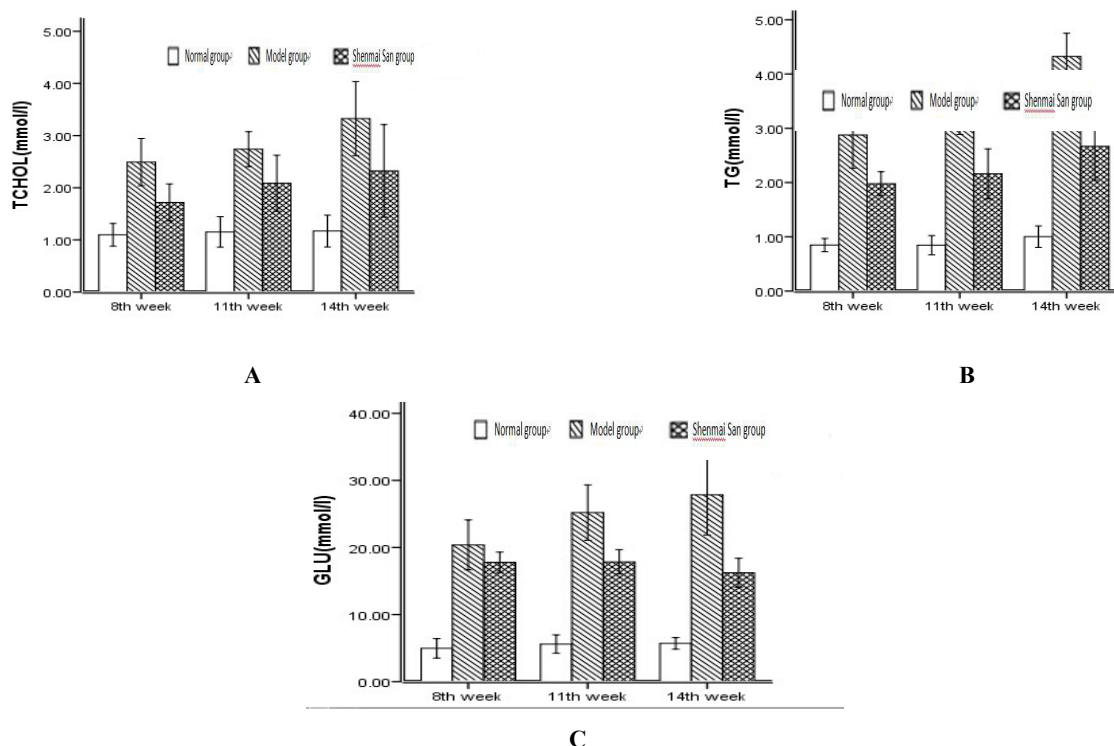


Figure 1. The changes of biochemical indexes of rats. A: The change of serum total cholesterol in rats; B: The change of blood glucose in rats; C: The change of serum triglyceride in rats.

Myocardial Injuries Observed by ECG

The ECG in rats showed obvious ST-segment elevation, indicating myocardium had been injured.

Pathological Observation

After the HE staining, neat myocardial cells with compact, clear structure, less extracellular matrix, and a small amount of fibroblasts could be seen in the normal rats (Figure 2-A); In the model group, disorderly

arranged myocardial cells, cardiomyocyte hypertrophy and distortion, enlarged cell gaps, increased interstitial and perivascular extracellular matrix, and increased number of fibroblasts with inflammatory cells infiltrated were shown (Figure 2-B); And in the Shengmai San group, the state was somewhat in between, and compared with the model group, narrowed cell gaps, and reduced interstitial and perivascular extracellular matrix were shown (Figure 2-C).

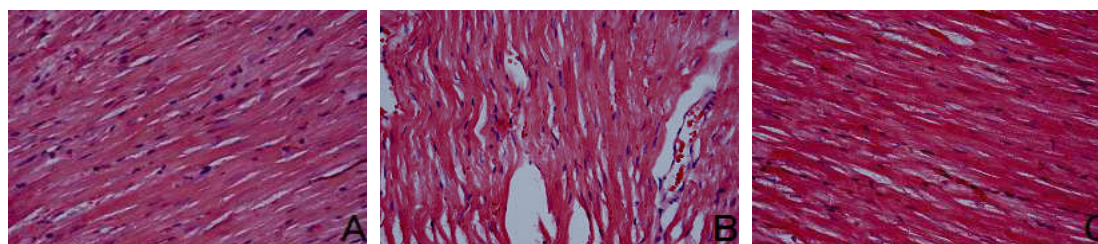


Figure 2. The myocardial HE staining of rats (200×). A: the normal group; B: the Model Group; C: the Shengmai San group.

Observation of Cardiac Subcellular Structures with Electron Microscope

In the normal group, normal arrangement of myocardial cells with clear structure, less collagen content in the extracellular matrix, normal capillary endothelial cells and normal basement membrane structure were shown (Figure 3-A); In the model group, sparse, distorted and broken myofilament fiber, swelling mitochondrial with decrease in mount, disorder arrangement, vacuolar degeneration, broken in a part of ridges and decreased

glycogen in the myocardial cells; and interstitial collagen hyperplasia, capillary endothelial cell swelling, capillary basement membrane thickening were shown (Figure 3-B); And in the Shengmai San group, compared with the model group, the lesion was significantly reduced with less interstitial collagen deposition and less thick capillary basement membrane, and the lesion degree was at between the normal group and the control group (Figure 3-C).

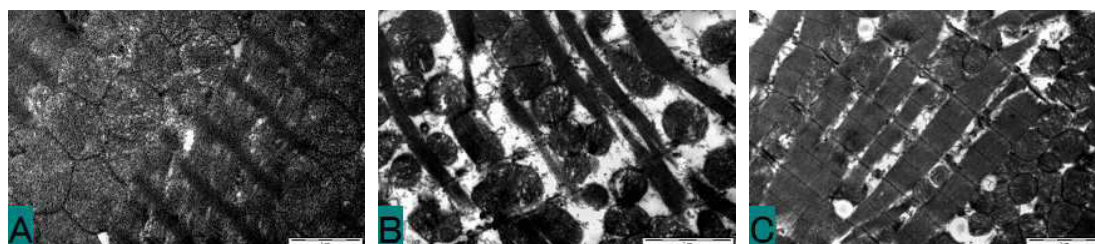


Figure 3. Observation of the myocardial tissue with electron microscope in different rat groups (15 000 ×). A: the normal group; B: the Model Group; C: the Shengmai San group

Masson Staining of Collagen Expression

Under the microscope, in the normal group, the distribution of collagen tissue was almost equal, the collagen fiber network among adjacent cells was intact with less collagen fiber content (Figure 4-A); in the control group, significantly increased myocardial collagen tissue, broken and disorderly arranged collagen fiber network around myocardial cells were shown (Figure 4-B); And in the Shengmai San group, compared with the control group, the arrangement of collagen tissue and the structure of the fiber network were better (Figure 4-C).

With the Image Pro Plus image analysis system, the relative content of collagen in myocardial tissue were measured and the result showed that compared with the normal group, the relative myocardial collagen content in the diabetic cardiomyopathy rat increased significantly ($P<0.01$), suggesting the existence of the lesion of collagen fiber hyperplasia in this rat model; Compared with the model group, collagen content in the Shengmai San group decreased significantly ($P<0.05$), suggesting that the Shengmai San can remarkably inhibit the proliferation of collagen fibers (Table 1).

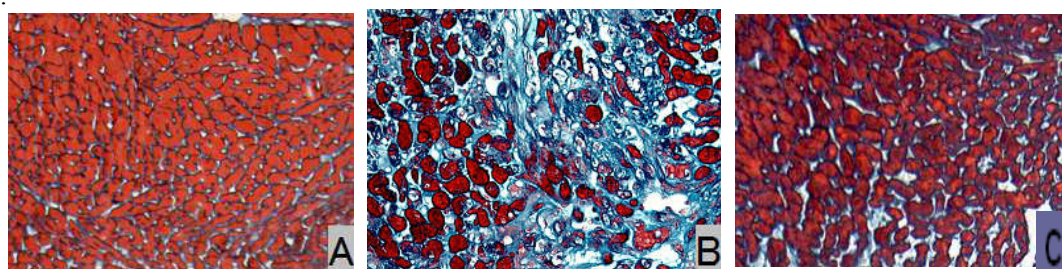


Figure 4. The Masson staining in rat myocardium (100 ×). A: the normal group; B: the model Group; C: the Shengmai San group

Table 1. The quantitative analysis on Masson staining of collagen fibers in rat left ventricular tissue of different groups ($\bar{x} \pm s$)

Groups	<i>n</i>	Volume of the interstitial collagen
Normal group	12	10.38±2.76
Model group	11	18.42±3.55 [△]
Shengmai San group	12	15.90±3.00*

Notes: Compared with the normal group, [△] $P<0.01$; Compared with the model group, * $P<0.05$. “*n*” stands for rats’ number.

Cell Apoptosis Detection with TUNEL Apoptosis Detection Kit

In the normal group, only a small number of rat myocardial cell apoptosis were seen (Figure 5-A).

However, compared with the normal group, the number of apoptotic cells significantly increased in the model group (Figure 5-B), and compared with the model group, apoptotic cells were significantly reduced in the Shengmai San group (Figure 5-C).

Real-time Fluorescence Quantitative PCR Detection

Compared with the normal group, the mRNA expression levels of TSP-1 and TRB-3 were significantly increased in the model group ($P<0.01$). Compared with the model group, the mRNA expression levels of TSP-1 and TRB-3 were significantly decreased in the Shengmai San group ($P<0.01$, Table 2).



Figure 5. The levels of rat myocardial cell apoptosis in different groups (200 ×). A: the normal group; B: the model Group; C: the Shengmai San group

Table 2. mRNA expression levels of TSP-1 and TRB-3 in the rat myocardium of different groups ($\bar{X} \pm s$)

Groups	<i>n</i>	TSP-1	TRB-3
Normal group	12	0.0091±0.0019	0.0081±0.0030
Model group	11	0.0144±0.0034 [△]	0.0136±0.0039 [△]
Shengmai San group	12	0.0122±0.0034 [*]	0.0102±0.0023 [*]

Notes: Compared with the normal group, [△] $P < 0.01$; Compared with the model group, ^{*} $P < 0.05$. “*n*” stands for rats’ number.

Immunohistochemistry

The positive TSP-1 staining signal was brown particles located in the cytoplasm of myocardial cells. In the

normal group, uniform distribution, sparse, light brown particles could be seen in the myocardial cells (Figure 6-A); in the model group, thick dark brown granules could be seen in the myocardial cells (Figure 6-B), and in the Shengmai San group, significantly decreased brown particles in the myocardial cells were visible (Figure 6-C). Compared with the normal group, the myocardial TSP-1 protein expression was significantly increased in the model group, and compared with the model group, the TSP-1 expression was significantly reduced in the Shengmai San group, with significant differences among the three groups (all $P < 0.01$).

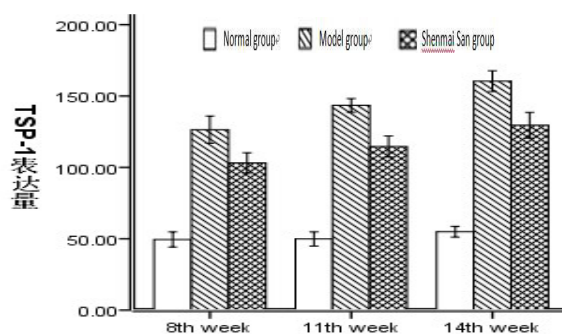
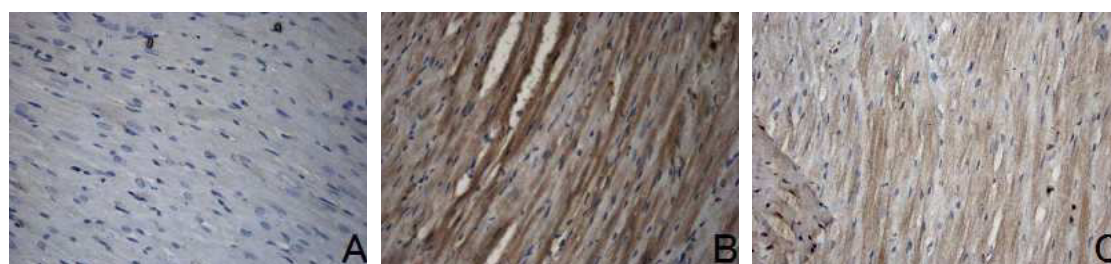


Figure 6. A,B,C: The TSP-1 expression in rat myocardium in different groups (200 ×). A: the normal group; B: the model group; C: the Shengmai San Group) and D: The quantities of expression of TSP-1 in different groups.

The positive TGF-β1 staining signal was brown particles located in the cytoplasm of myocardial cells. In the normal group, scattered, sparse, light brown particles could be seen in the myocardial cells (Figure 7-A); in the model group, thick dark brown granules could be seen in the myocardial cells (Figure 7-B), and in the Shengmai San group, significantly decreased brown particles inside

the myocardial cells were visible (Figure 7-C). Compared with the normal group, the myocardial TGF-β1 protein expression was significantly increased in the model group, and compared with the model group, the TGF-β1 expression was significantly reduced in the Shengmai San group, with significant differences among the three groups (all $P < 0.01$).

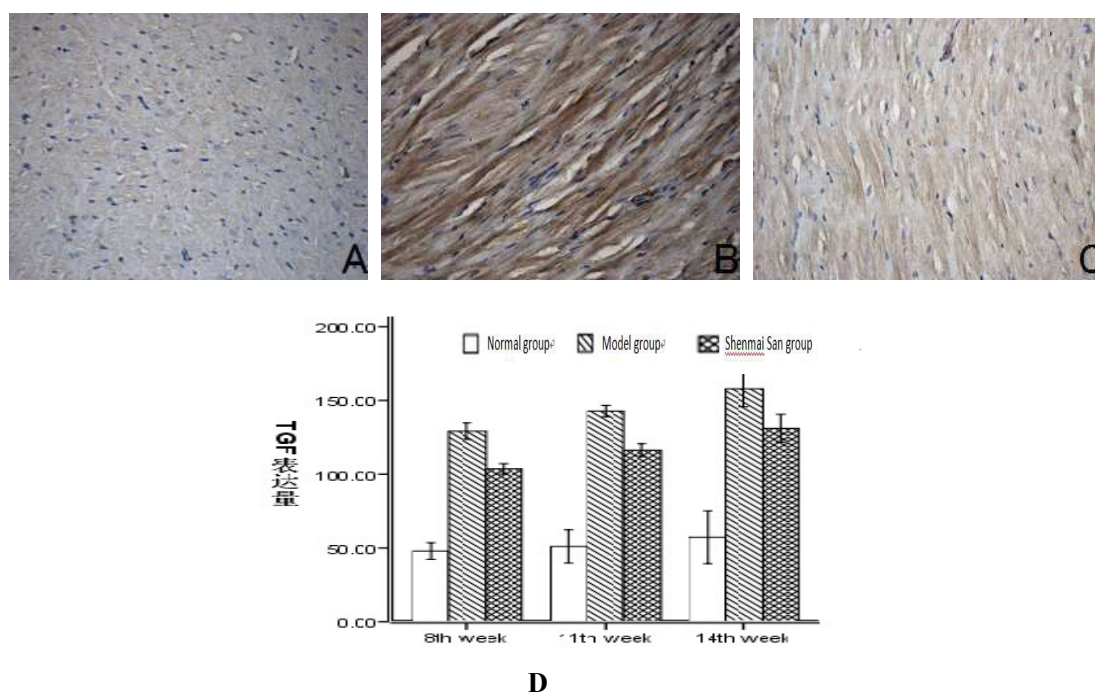


Figure 7. A,B,C: The TGF- β 1 immunohistochemistry in rat myocardium in different groups (200 \times). A: the normal group; B: the model group; C: the Shengmai San Group and D: The quantities of expression of TGF in different groups.

The positive TRB-3 staining signal was brown particles located in the cytoplasm of myocardial cells. In the normal group, scattered, sparse, light brown particles could be seen in the myocardial cells (Figure 8-A); in the model group, thick dark brown granules could be seen in the myocardial cells (Figure 8-B), and in the Shengmai San group, significantly decreased brown particles in the

myocardial cells were visible (Figure 8-C). Compared with the normal group, the myocardial TRB-3 protein expression was significantly increased in the model group, and compared with the model group, the TRB-3 expression was significantly reduced in the Shengmai San group, with significant differences among the three groups (all $P < 0.01$).

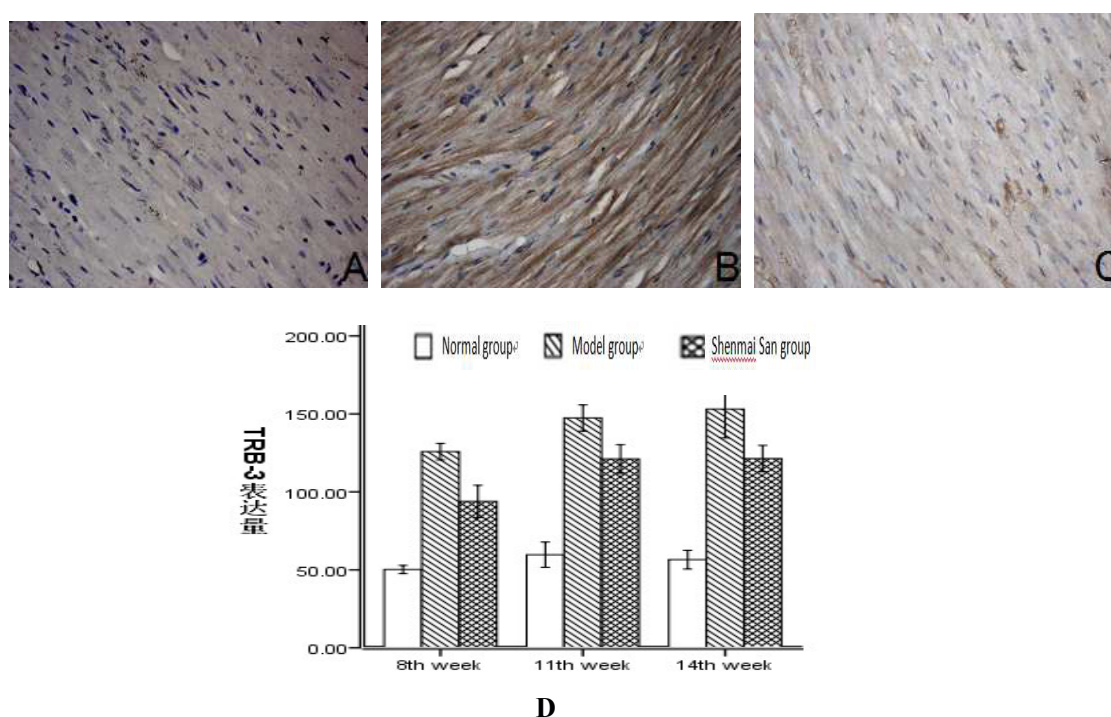


Figure 8. A,B,C: The TRB-3 immunohistochemistry in rat myocardium in different groups (200 \times). A: the normal group; B: the model group; C: the Shengmai San Group and D: The quantities of expression of TRB-3 in different groups.

The positive Chymase staining signal was brown particles. In the normal group, scattered, sparse, light brown particles could be seen in the gaps of myocardial cells and mastocytes (Figure 9-A); in the model group, thick dark brown granules could be seen in the gaps of myocardial cells and mastocytes (Figure 9-B), and in the Shengmai Pulvis group, significantly decreased brown particles in the gaps of myocardial cells and mastocytes

were visible (Figure 9-C).

The myocardial Chymase protein expression was significantly increased in the model group; Compared with the model group, the Chymase expression was significantly reduced in the Shengmai San group, with significantly differences among the three groups (all $P<0.01$).

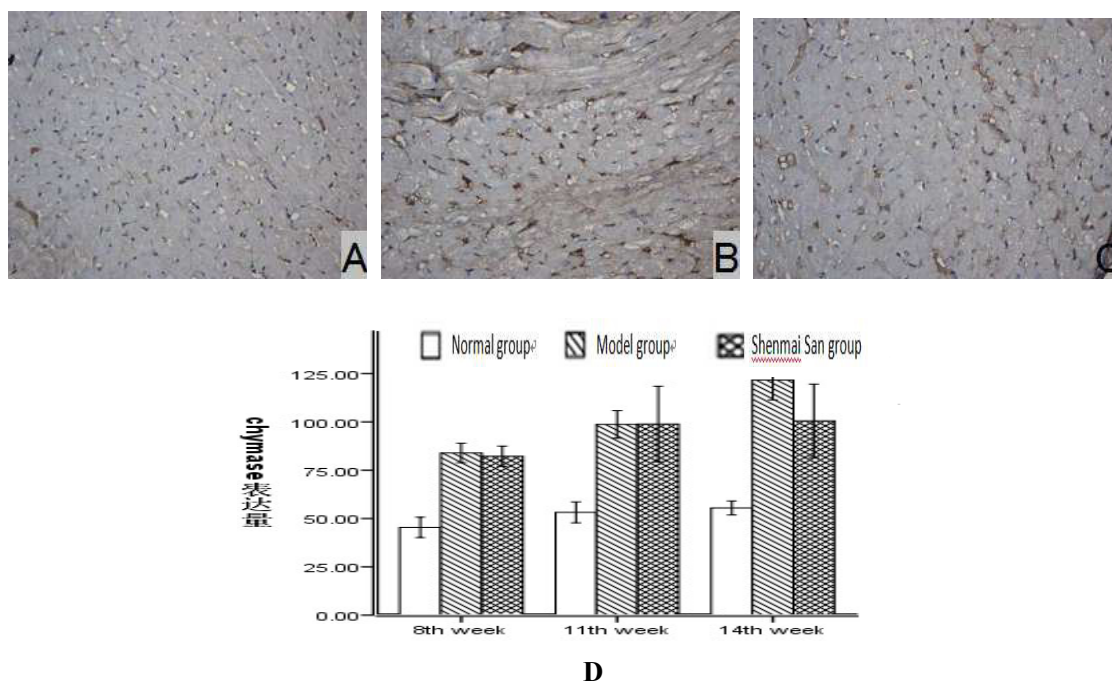


Figure 9. A,B,C: The Chymase immunohistochemistry in rat myocardium in different groups (200 ×). A: the normal group; B: the model group; C: the Shengmai San Group and D: The quantities of expression of Chymase in different groups.

Western Blot Detection of Protein Expression

The TGF- β 1 in myocardium exists in two forms, one is A-TGF- β 1 with activity and the other, L-TGF- β 1 with non-activity. Compared with the normal group, expression levels of the three proteins TSP-1, A-TGF- β 1, L-TGF- β 1 in the myocardial tissue were significantly

higher than those in both the model group and the Shengmai San group (all $P<0.01$). Compared with the model group, the expression levels of the three proteins TSP-1, A-TGF- β 1, L-TGF- β 1 were significantly lower than those in the Shengmai San group ($P<0.05$ or $P<0.01$, Table 3)

Table 3. Expression levels of TSP-1, A-TGF- β 1 and L-TGF- β 1 in the rat myocardium in the groups ($\bar{x} \pm s$)

Groups	<i>n</i>	TSP-1	A-TGF- β 1	L- TGF- β 1
Normal group	12	93.2 \pm 5.4	106.4 \pm 6.3	102.4 \pm 6.1
Model group	11	129.7 \pm 6.5 [△]	139.8 \pm 7.2 [△]	144.6 \pm 7.4 [△]
Shengmai San group	12	123.3 \pm 6.7*	129.7 \pm 6.3*	129.8 \pm 7.6*

Notes: Compared with the normal group, [△] $P<0.01$; Compared with the model group, * $P<0.05$. "n" stands for rats' number.

DISCUSSION

In this study, the animal model established by combination of insulin resistance induced by high sugar, high fat and high calorie diet, with low-dose STZ injection, was basically consistent with the clinical features of diabetes, including pathological cardiomyocyte hypertrophy and distortion, enlarged

intercellular space, increased intercellular substance and extracellular matrix around blood vessels; and sparse arrangement and rupture of myocardial cells with a lot of collagen fibers, as well as myocardial damage. It is suggested that in this research the animal model of diabetic cardiomyopathy is successfully established. Shengmai San, which originated from the work,

"*Medical Origins*", written by Zhang Yuansu, a physician in Jin dynasty, consists of three traditional Chinese herbs, Ren Shen (Radix Ginseng) 9 g, Mai Dong (Radix Ophiopogonis) 9 g, and Wu Wei Zi (Fructus Schisandrae) 6 g. It is a commonly-used prescription for treating the syndrome of *Qi-Yin* deficiency. In recent years, it has been commonly used for treatment of the diseases with *Qi-Yin* deficiency syndrome including acute myocardial infarction or coronary heart disease, etc. Recent studies show that Shengmai San can improve fat metabolism. Liao, et al.¹⁰ found in a study that the levels of TC, TG and LDL-C of the animal fed by high-fat diet were decreased and the level of HDL-C was increased in the Shengmai San group, indicating that Shengmai San can regulate lipid metabolism, improve blood circulation and microcirculation, increase endurance to hypoxia. Thus it has a good effect on hyperlipidemia and cardiovascular disease.

Diabetic cardiomyopathy is characterized mainly by cardiac hypertrophy, a significant reduction in myocardial cells, myocardial interstitial and perivascular fibrosis, sediment of a large number of glycogen and lipid droplets, calcium transport defects in cellular levels, and collagen formation of myocardial contractile protein. Microvascular myocardiopathy and abnormal cardiac metabolism can cause myocardial ischemia and hypoxia, and further diffuse small focal myocardial necrosis and the gradual formation of fibrous lesions, with the increase in myocardial stiffness, the cardiac function gradually deterioration, and eventually lead to the occurrence of diabetic cardiomyopathy, which therefore fundamentally manifested as myocardial hypertrophy and interstitial fibrosis in the myocardial cells. Though, in the past, diabetic cardiomyopathy is thought mainly be due to proliferation and hypertrophy of the myocardial cells. However, in recent years, it has been recognized that the non-cardiac cells which accounts for 2/3 of heart cells (fibroblasts is main) and extracellular interstitium (major component is myocardial collagen) play essential roles in the ventricular remodeling. Cardiac interstitium, perivascular fibrosis and local micro-scar formation can lead to cardiac hypertrophy, heart dysfunction, and eventually heart failure.

This experiment showed that in the normal group myocardial cells arranged in neat dense rows with smaller intracellular spaces, and the Masson staining showed that only a small amount of collagen fibers could be found between myocardial cells; electron microscope observation indicated that cardiomyocytes arranged in neat rows with integrated mitochondria, and under low magnification (1250 \times), fibroblasts were fewer (≤ 2), with a less collagen fibers around fibroblasts. Compared with the normal group, in the model group myocardial fibroblasts arranged disorderly, with increased cell gaps, and the Masson staining showed that a lot of collagen fibers were observed between myocardial cells; fracture

and collapse of filaments in the cardiomyocytes, and swelling and rupture of mitochondria could be found with electron microscope; and under low magnification (1250 \times), fibroblasts were more (≥ 5), and a lot of collagen fibers accumulated around fibroblasts. For the Shengmai San group, the state was somewhat in between. Compared with the model group, myocardial cells arranged in relatively neat rows with relatively decreased cell gaps in the Shengmai San group, and the Masson staining showed that a lot of collagen fibers were observed between myocardial cells; fracture and collapse of filaments in the cardiomyocytes, and swelling and rupture of mitochondria could be found with electron microscope; and, under low magnification (1250 \times), numbers of fibroblasts were about 2-4, and a moderate amount of collagen fibers accumulated around the fibroblasts, indicating that Shengmai San can effectively delay the process of the occurrence of diabetic cardiomyopathy.

This study is on the several key cytokines in fibrosis process, observing the protective function of Shengmai San in diabetic cardiomyopathy, and providing evidence for the wide clinical application. TSP-1 has a strong regulatory function for differentiation and proliferation in multiple interstitial cells, and its abnormal expression plays a key role in the process of fibrotic diseases of various types.¹¹ TGF- β 1 is a multifunctional regulator of cell activity and plays an important role in embryogenesis, immune regulation, wound healing, fiber generation and cell apoptosis. It exists in almost all tissues, TGF- β 1 and its receptor can be expressed in both the myocardial cells and the non-myocardial cells of the heart, which is the key mediator of myocardial fibrosis. TGF- β 1 in the myocardial cells exists in two forms, namely, activated TGF- β 1 (A-TGF- β 1) and latent TGF- β 1 (L-TGF- β 1). L-TGF- β 1 is a protein complexes formed by Latency-associated peptide (LAP) and TGF- β 1 in 1:1 ratio by non-covalent combination, which can not combine with TGF- β 1 receptors and therefore TGF- β 1 can not perform the biological activity.

TSP-1 can combine with the N-terminal of LAP, leading to the cleavage of LAP and TGF- β 1, so as to further activate TGF- β 1. High blood sugar and AGEs (advanced glycation end-products), as the upstream activator of TSP-1, can activate the TSP-1, inducing the activation of TGF- β 1, and further leading to the formation of myocardial fibrosis and diastolic dysfunction of the left ventricle, eventually the occurrence of diabetic cardiomyopathy. Studies has shown that the glucose/TSP-1/TGF- β 1 signal transduction pathway plays an important role in the process of the occurrence and development of myocardial interstitial fibrosis in diabetic cardiomyopathy,¹² indicating that TSP-1 is not only an important physiological activator of TGF- β 1, but also the primary activator for TGF- β 1 inducing myocardial fibrosis. Therefore, a lasting expression of

TSP-1 has a positive-feedback function for the biological activity of TGF- β 1 in cardiac fibroblasts. The mechanism of TRB3 involved in myocardial fibrosis of diabetic cardiomyopathy is not clear yet, but a recent research on TRB3 signal transduction pathway shows that TRB3 has a broad and specific regulatory function on the chain reaction of MAPK signal transduction pathway, and the combination of TRB3 with the MAPKK can regulate the activity of signal proteins in the MAPK pathway.^{13,14}

A large number of studies confirm that MAPK is not only a key cell factor for the onset and development of diabetic complications, such as diabetic nephropathy, diabetic atherosclerosis, etc.,¹⁵⁻¹⁷ but also an important signal transduction pathway for myocardial fibrosis.^{18,19} Chymase, found in 1953, is a chymotrypsin-like serine proteases, which exist widely in organs, including the heart, blood vessels, the lungs and skin, etc. Studies confirm that chymase provides more than 80% angiotensin II (Ang II) source for the heart, and the biological activity of chymase-sourced Ang II is about 20 times that of the ACE-sourced; while the role of Ang II in the development of diabetic cardiomyopathy is now drawing more and more attention. Under a diabetic condition, increase of local myocardial Ang II can cause myocardial oxidative stress, apoptosis, myocardial interstitial collagen deposition and myocardial fibrosis through multiple ways, playing an important role in the occurrence of diabetic cardiomyopathy.²⁰ In addition, Chymase may also directly activate TGF- β 1 to induce cell proliferation and promote myocardial fibrosis.²¹

The experimental results showed that compared with the normal group, for Masson staining, the expression of collagen fibers in the model group increased, and the expression of collagen fibers around fibroblasts increased under electron microscope; immunohistochemistry showed that the expression levels of TSP-1, TGF- β 1, chymase, and TRB-3 in myocardial cells were significantly increased to different extents in the model group ($P < 0.01$). Compared with the model group, the expression levels of TSP-1, TGF- β 1, chymase, and TRB-3 in myocardial cells were significantly decreased to different extents in the Shengmai San group, in combination with the results of Masson staining and electron microscopy, it is indicated that Shengmai San can effectively delay the process of myocardial fibrosis of diabetic cardiomyopathy, and alleviate the extent of fibrosis of diabetic cardiomyopathy. The results of semi-quantitative Western blotting showed that compared with the normal group, the expression levels of TSP-1, A-TGF- β 1 and L-TGF- β 1 were significantly increased in the model group, and the results of quantitative PCR showed that compared with the normal group the mRNA expression levels of TSP-1 and TRB-3 were increased in the model group. All the results above indicate that the expression levels of the key factors in the fibrosis process of rat myocardial tissue in diabetes were

significantly increased at both gene expression and protein expression levels. The expression of L-TGF- β 1 of non-activity is still elevated, though it does not directly involved in the process of fibrosis in diabetic cardiomyopathy, which is consistent with other studies, partly due to increased gene expression of TGF- β 1 that may further lead to increase of expression of L-TGF β 1. Compared with the model group, the expression levels of TSP-1, A-TGF- β 1 and L-TGF- β 1 were decreased in the Shengmai San group, indicating that Shengmai San may delay the occurrence of cardiac fibrosis by reducing the expression of cytokines in the process of fibrosis.

REFERENCES

1. Rullber S, Dulgush J, Yuceogl YZ, Kumral T, Branwood AW, Grishman A. New type of cardiomyopathy associated with diabetic glomerulosclerosis. *Am J Cardiol* 1972; 30: 595-602.
2. Hamby RI. Diabetic cardiomyopathy. *JAMA* 1974; 229: 17492-17493.
3. Paul Poirier, MD, FRCPC, Peter Bogaty. Diastolic Dysfunction in Normotensive Men with Well-Controlled Type 2 Diabetes: Importance of maneuvers in echocardiographic screening for preclinical diabetic cardiomyopathy. *Diabetes Care* January 2001; 24: 5-10.
4. Schannwell CM. Left ventricular diastolic dysfunction as an early manifestation of diabetic cardiomyopathy. *Cardiology* 2002; 98: 33-30.
5. Mizushige K, Yao L, Noma T, Kiyomoto H, Yu Y, Hosomi N, et al. Alteration in left ventricular diastolic filling and accumulation of myocardial collagen at insulin-resistant prediabetic stage of a type II diabetic rat model. *Circulation* 2000; 101: 899-907.
6. Asbun J, Villarreal FJ. The pathogenesis of myocardial fibrosis in the setting of diabetic cardiomyopathy. *J Am Coll Cardiol* 2006; 47: 693-700.
7. Cai L, Wang Y, Zhou G, Chen T, Song Y, Li X, et al. Attenuation by metallothionein of early cardiac cell death via suppression of mitochondrial oxidative stress results in a prevention of diabetic. *Cardiol* 2006; 48: 1688-1697.
8. Martin J, Kelly DJ, Mifsud SA, Zhang Y, Cox AJ, See F, et al. Tranilast attenuates cardiac matrix deposition in experimental diabetes: role of transforming growth factor-beta. *Cardiovasc Res* 2005; 65: 694-701.
9. Sowers JR, Epstein M, Frohlich ED. Diabetes, hypertension, and cardiovascular: an update. *Hypertension* 2001; 37: 1053-1059.
10. Liao ZY, Jiang JL, Liu H. Effects of Shengmai San on experimental hyperlipidemia, hemorheology and antioxidation in rats. *Liaoning. J Tradit Chin Med (Chin)* 2007; 34: 1478-1479.
11. Morishima Y, Nomura A, Uchida Y. Triggering the induction of myofibroblast and fibrogenesis by airway epithelial shedding. *Am J Respir Cell Mol Biol* 2001; 24: 1-11.
12. Zhong M, Zhang W, Miao Y, Ma X, Gong HP, Sun H, et al. The role of glucose / TSP-1 / TGF β 1 signal pathways in diabetic cardiomyopathy. *Chin J Cardio (Chin)* 2006; 34: 217-220.

13. Kiss-toth E, Bagstaff SM, Sung HY, Jozsa V, Dempsey C, Caunt JC, et al. Human Tribbles, a Protein family controlling mitogen-activated Protein kinase cascades. *J Biol Chem* 2004; 279: 42703-42708.
14. Sung H.Y., Francis S.E., Crossman D.C, Kiss-Toth E. Regulation of expression and signaling modulator function of mammalian tribbles is cell-type specific. *Immunology Letters* 2006; 104: 171-177.
15. Stmiskova M, Baraneik M, Neekar J. Mitogen-activated Protein kinases in the acutediabe-tiemyocardium. *Mol Cell Biochem* 2003; 249: 59-65.
16. Purves T, Middlemas A, Agthong S. A role for mitogen-activated protein kinases in the etiology of diabetic neuropathy. *The FASEB J* 2001; 15: 2508-2514.
17. Ling L, Sawamura Tatsuya, RENIER Geneviève. Glucose enhances human macrophage LOX-1 expression: Role for LOX-1 in glucose-induced macrophage foam cell formation. *Circ Res* 2004; 94: 892-890.
18. Park JK, Fischer R, Dechend R, et al. P38 mitogen-activated protein kinase inhibition ameliorates angiotensin II-induced target organ damage. *Hypertension* 2007; 49: 481-489.
19. Saka Masako, Obata Koji, Ichihara Sahoko, et al. Attenuation of ventricular hypertrophy and fibrosis in rats by pitavastatin: Potential role of the RhoA-extracellular signal-regulated kinase-serum response factor signalling pathway. *Clin Exp Pharmacol Physiol* 2006; 33: 1164-1171.
20. Cong L, Yu MH, Li YM. Chymase and diabetic cardiomyopathy. *Foreign Medicine. Endocrinology (Chin)*. 2004, 24: 33-35.
21. Zhao XY, Zhao LY, Zheng QS, He YP, Lu XL. Effects of Chymase on cardiac fibroblast proliferation and collagen synthesis. *Heart (Chin)* 2008; 20: 268-272.

(Received March 30, 2011)